Radiation damage of LHCb electromagnetic calorimeter

(to be submitted to NIM)

S.Barsuk, A.Golutvin, V.Kirichenko, I.Korolko, S.Malyshev, V.Rusinov and E.Tarkovski

ITEP, Moscow

Abstract

Addressed is an extensive irradiation test program carried on to establish proper design and materials to build electromagnetic calorimeter that matches radiation conditions of the LHCb experiment at CERN. The results obtained are compared with measurements by other groups.

1 Introduction

"Shashlik" calorimeter technology, implying a sampling scintillator/lead structure read out by plastic WLS fibers, has been accepted for electromagnetic calorimeter production in the LHCb experiment [1]. This decision was made taking into account good energy resolution, fast response time and reliability of the "shashlik" technology, as well as the experience accumulated at other experiments [2, 3, 4].

Below the emphasis is made on irradiation test results and comparison to those from other groups in view of LHCb calorimeter design and materials to be established.

2 LHCb electromagnetic calorimeter

LHCb detector is aimed at the precision study of CP asymmetries in B meson system, and rare B decays, exploiting the LHC potential as a copious source of b flavour hadrons. The experiment will operate with an average luminosity of $2 \times 10^{32}\ cm^{-2}s^{-1}$ and achieve the production rate of $10^{12}\ b\bar{b}$ pairs per year of data taking.

$B_d^0 \to \rho^0\pi^0 \oplus tag$, $B_d^0 \to \rho^+\pi^- \oplus tag$, $B_d^0 \to J/\psi K_S^0 \oplus tag$, $B_d^0 \to K^{*0}\gamma$ and $B_s^0 \to J/\psi\phi \oplus tag$ are the decays that illustrate the role of electromagnetic calorimeter in the LHCb experiment. Efficient π^0's reconstruction in the wide range of momentum spectrum, discrimination between electrons and charged hadrons with overlapping photons, the tag electron and high energy γ reconstruction contribute a good deal of the scientific program to the experiment.

Electromagnetic calorimeter is a part of LHCb calorimeter system, which also comprises the preshower detector (used to improve the h/e separation) and the hadron calorimeter. Electromagnetic calorimeter will be placed at about 12.5 m from the interaction point (Figure 1). The readout system of the calorimeter comprises 5952 channels, 1472, 1792 and 2688 from which belong to inner, middle and outer regions respectively.

The physics tasks impose the following requirements on the performance of the LHCb calorimeter.

- **Acceptance.** The outer dimensions match projectively to those of the tracking system, $\theta_x < 300\ mrad$ and $\theta_y < 250\ mrad$. Due to the substantial radiation dose level around the beam pipe, the active calorimeter volume has a central square hole of $65 \times 65\ cm^2$.
- **Response time.** The time between two subsequent bunches at LHC is 25 ns. Thus to avoid event pile-up, signal collection must proceed well within this time interval.
- The hit density is a steep function of the distance from the beam pipe, and varies

over the active calorimeter surface by two orders of magnitude. The **transverse segmentation** is optimized on the basis of best possible π^0 reconstruction efficiency and trigger performance, with a constraint of the maximum allowed cost of calorimeter (mainly determined by the number of cells). Calorimeter is subdivided into three, inner, middle and outer, regions, with the $40.4 \times 40.4\ mm^2$, $60.6 \times 60.6\ mm^2$ and $121.2 \times 121.2\ mm^2$ cell size respectively.

- The design **energy resolution** of

$$\frac{\sigma_E}{E} = \frac{10\%}{\sqrt{E}} \oplus 0.8\% \quad (E\ in\ GeV)$$

provides e/h separation at a level better than 100 and is adequate for π^0 reconstruction.

- **Radiation conditions.** The annual radiation dose is as much as [1] $0.25\ Mrad$ for the innermost modules and drops drastically with the distance from the beam axis (see Figure 2). The longitudinal dose profile for the innermost module is plotted in Figure 3, where the contributions from electromagnetic and hadronic components of the shower are shown separately. The radiation mostly affects relatively small part of the calorimeter in the vicinity of shower maximum. The modules of middle and outer regions do not suffer from such a dose, the maximum dose achieves here about $0.02\ Mrad$ per year of LHCb operation. The radiation resistance of the LHCb electromagnetic calorimeter modules, as well as of the module components, is discussed below.

3 Module design

The schematic drawing of LHCb calorimeter modules is shown in Figure 4. Inner, middle and outer section modules have similar design differing by the number of cells per module and by the fiber density. We are planning to use 9, 4 and 1 cells per

[1] Note the difference with respect to [1].

calorimeter module and 16, 36 and 64 fibers [2] per cell for the inner, middle and outer regions respectively.

Each module is constructed from alternating layers of 2 mm thick lead, white reflecting 120 μ thickness paper (TYVEK) and 4 mm thick scintillator tiles.

The tile is produced of polystyrene-based PSM-115 scintillator with the 2.5% p-terphenyl and 0.01% $POPOP$ admixtures. The concentration of scintillating dopants is chosen so, that the scintillator light is almost saturated, and is tuned for the scintillator emission spectrum to match the absorption spectrum of WLS fiber. Scintillator tile production employs the high pressure injection moulding technique.

Tile edges are mat [3] in order to improve light collection and prevent tile-to-tile light crosstalk. Alternatively the tile edges could be aluminized (HERA-B solution) with the technique of Al evaporation in vacuum by HV-induced explosion [4].

Complete stack is compressed using stainless steel side covers of 100 μ thickness, pretensioned and welded to front and rear steel lids. In sum, there are 66 layers resulting in a total depth of 25 X_0.

The light is read out via 1.2 mm diameter WLS fibers penetrating the entire module, with PM. The fibers belonging to each calorimeter cell are bundled at the end of the module and polished. The fibers form a loop in the front part of the module for large tower sizes, where loop is possible without significant light losses. Such fiber "pairing" is not possible for small tower sizes (small curvature radii of fibers), i.e. for inner section modules. In this latter case, the fibers are cut, polished, and aluminium mirror is made on the fiber front edge.

[2] For fiber density choice considerations see [5].

[3] Tile edge coverage is discussed in detail in [5].

[4] Slightly ($\sim 10\%$) worse reflection quality is achieved with this method.

4 Radiation damage studies

As long as the photostatistics is sufficient (for LHCb ECAL we expect to have about 1000 $p.e./GeV$), energy resolution is determined by sampling term and design specifity of the module. Among the calorimeter components active are plastic (scintillator and WLS fibers) and PM. Under irradiation their properties change. Below only scintillator [5] and WLS fibers damage is discussed. Other components damage – degradation of mirror at the fiber front edge [6], light mixer and PM window transparency deterioration, etc. – is not discussed here.

The deterioration of plastic leads to the light yield reduction and energy resolution degradation. The former effect is not critical, because photostatistics contribution to the energy resolution remains negligible. Namely the latter effect stimulates intense interest to the radiation problem studies. Radiation induced transverse and longitudinal non-uniformity makes the constant term rising.

At present many radiation test results are available. Measurement conditions of each test are to the utmost fit to the specific experiment, under the same accumulated dose they differ by

- the dose parameters (dose rate, dose profile);
- annealing time (time interval between the irradiation and the measurement);
- particles used for irradiation (photons, electrons, charged hadrons, neutrons);
- scintillator (wide-spread are $PSM-115$ and $SCSN-81$);

[5] As far as the scintillator is concerned, studied is the integral effect of brightness, transparency and possible tile edge coverage degradation.

[6] Recent Monte Carlo studies showed radiation dose in this region to be higher than expected from early calculations, compare starting point in Figure 3 to that in Figure 10.7 from [1]. Since the inner section modules will be built at a later stage of production, the exact solution on mirrors will be studied and presented in 2001.

- fiber type (Kuraray $Y11$, Bicron $BCF91$, $BCF92$ and $BCF99$, Pol.Hi.Tech. $S048$ and $S248$; single or multi-cladding);
- geometrical features (fiber and tile dimensions, fiber density, module geometry, etc.).

Let us briefly discuss the **experience accumulated by previous experiments**. Radiation induced damage reduces both brightness (abilities to emit light for scintillator, and to re-emit light for fibers) and transparency of scintillator tiles and WLS fibers.

Brightness deterioration is first of all the property of materials themselves, and is considered to substantially depend on the irradiation method, in particular, on the dose accumulation rate and particle type. This effect is thought to take place, because the annealing process proceeds in parallel with the radiation induced degradation. Thus under small dose rate, one expects competing annealing process to noticeably compensate the degradation. So far radiation tests were carried out with the dose rates, that were considerably higher compared to those expected in the experiment.

Similar to brightness deterioration, the change in mean path of photons depends on material and irradiation method, but also is a strong function of the pattern geometry. For scintillator this means, that the less the initial mean light path the less radiation induced changes will take place. Thus, in order of "Shashlik" type calorimeter to operate in the highly irradiated area, profitable is the use of small size tiles and high fiber density, to diminish the initial mean light path.

For fiber damage studies important are the dose irradiation profile (uniform or approximated according to the expected distribution), and the coverage quality of front edge of the fiber [7]. Another critical parameter, fiber length, is considered to equal to 0.5 m, typical for LHCb electromagnetic calorimeter, for further discussion.

[7] Using mirror increases signal from the very front part of the module, where the major degradation takes place, almost twice, depending on the mirror quality. At the same time light originated near the PM side of the module, is actually not changed because the extra-light twice goes through the region of shower maximum. Thus it reduces the radiation induced effect of longitudinal non-uniformity.

Major part of experiments aimed at radiation hardness studies of plastic materials used radioactive sources for irradiation. Complete module irradiation with the electron beam [6, 7] qualitatively showed the picture similar to that after irradiation with the source. Along with that, the irradiation with the proton beam [8] demonstrated possible dependence of the damage on particle type used for irradiation.

All the aspects discussed above, explain the difficulties arises when extrapolating the information available to the LHCb conditions. Required is either additional assumptions or dedicated radiation test program. Nonetheless the information available allowed to make the **preliminary material selection** for further detailed testing.

Important for scintillator material pre-selection is [9], where authors concluded that in view of brightness and radiation hardness the combination of $PSM-115$ plastic and $Y11$ fibers is about equivalent to that of $SCSN-81$ plastic and the same $Y11$ fibers, so that the two major scintillator types, $PSM-115$ and $SCSN-81$, show similar performance. Scintillator damage of $PSM-115$ is illustrated by e.g. [10], where the emission spectrum of $PSM-115$ is compared to the degradation of scintillator transparency with respect to the wavelength of light.

The initial choice of $Y11-200(MS)$ [8] and $BCF-91A(DC)$ [9] fibers for detailed testing relies on the previous convincing measurements [10]. The illustrations of the measurements are briefly mentioned below. Bicron $BCF-99$ fibers showed clearly worse performance vs. radiation dose behaviour being studied with ITEP accelerator. $BCF99$ fibers degradation dynamics relative to the degradation of $BCF91$ fibers under irradiation [11] up to 0.5 $Mrad$ is shown in Figure 5. The light yield from the beam induced signal was monitored for $BCF-91A(DC)$, $BCF-99$ and $Y11-200(MS)$

[8] $Y11-200(MS)$ denotes multi-cladding (M) S-type (S) $Y11$ Kuraray fibers with the concentration of WLS dye of 200 ppm. S-type fiber core has molecular orientation along drawing direction, that makes the fiber mechanically stronger against cracking.

[9] $BCF-91A(DC)$ stands for double cladding (DC) $BCF-91A$ Bicron fibers.

[10] For LHCb time conditions acceptable among the Bicron products are faster $BCF-92A(DC)$ fibers, which from the other hand are measured to degrade significantly under irradiation.

[11] Particles from interactions of 2.5 GeV/c momentum proton beam with the target were used for irradiation.

fiber samples. Relative light yield ($\frac{LY\ (BCF99)}{LY\ (BCF91)}$) follows beam current curve, and annealing effect is clearly seen under no beam available. Unlike evident $BCF-99$ fiber degradation, $BCF-91A(DC)$ and $Y11-200(MS)$ fiber samples show similar behaviour at these dose conditions. This conclusion is in good agreement with e.g. [11]. Papers [11] and [12] show Pol.Hi.Tech. fibers also to be clearly worse than Kuraray products. Bicron $BCF-92A$ fibers also show worse radiation resistance [11, 12, 13].

Perfect experiment to answer all the questions concerned radiation damage would require proper beam (beam energy, beam composition), proper dose (including the rate similar to what is expected at LHCb), and a proper testing module. Unfortunately such an experiment run into many difficulties, e.g. it takes exactly an LHCb operation time. Still natural source of information mostly satisfying the above requirements is the electromagnetic calorimeter working in the HERA-B experiment. The dose conditions and module design of middle and outer parts of the HERA-B calorimeter are very much like those for inner and outer parts of LHCb .

5 Radiation test at LIL

An important radiation test has been carried out with LIL (LEP Injector Linac) accelerator at CERN. Three identical towers of $40 \times 40\ mm^2$ size [12] were assembled using $PSM-115$ plastic tiles and two species of fibers, $Y11-200(MS)$ and $BCF-91A(DC)$. Fibers had no treatment at their front end, so that only negligible fraction of reflected light from fiber front end, achieves PM. Tower represents a special sandwich of 20 layers each consistent of one 1.5 mm thick lead plate and five 4 mm thick scintillator tiles, in order to approximate combined electromagnetic and

[12] This size is close to that of LHCb inner section modules. Radiation resistance is critical for highly irradiated zone around the beam pipe, so that we experimentally study it for inner modules only. Outer section modules do not suffer from such a dose, thus having moderate requirements to their radiation resistance.

hadron dose profile [13] from [1], which will take place at LHCb , with 500 MeV energy electrons [14]. Two modules were irradiated with electrons of 500 MeV energy up to 5 $Mrad$ dose at shower maximum. The irradiation rate was approximately 10 rad/s (this should be compared to 0.05 rad/s maximum expected dose rate at LHCb).

Analyzed were irradiated modules with $Y11-200(MS)$ and $BCF-91A(DC)$ fibers, with respect to the reference non-irradiated module. Combining irradiated lead/scintillator stack with reference fibers, and reference lead/scintillator stack with irradiated fibers, one separates the damage effects of scintillator tiles and WLS fibers. Each combination was longitudinally scanned with ^{90}Sr radioactive source, and the light yield was measured. The main results obtained are discussed below.

Scintillator degradation and annealing effect after irradiation up to 5 $Mrad$ dose at shower maximum is shown in Figure 6. Plotted is the light yield vs. distance to PM in 7, 55, 175 and 2000 $hours$ after irradiation. Annealing effect is clearly seen up to ~ 50 $hours$ after irradiation. Annealing effect was also studied in [13] [15], and is in qualitative agreement with Figure 6. Dependence of scintillator damage on the dose rate was studied in [15], authors conclude, that degradation clearly increases with the dose rate.

Figure 6 reflects total signal reduction because of brightness degradation from one hand, and of light collection degradation, caused by scintillator blur, from the other. Light collection efficiency and its radiation induced degradation depend on [16] the attenuation length λ_{bulk}, which reflects a property of material to be transparent to the light of a given wavelength, and on the light absorption length λ_{geom} driven by the geometry (effective fiber surface, as seen by the light, and efficiencies of reflection from the tile edges, from the fiber holes and from TYVEK, enter λ_{geom}). λ_{bulk} worsens with

[13] The price for such tricky sandwich is the impossibility to directly measure overall module effect from irradiation.

[14] In [14] working scintillator tile/WLS fiber module was irradiated with 500 MeV energy electron beam, without real dose profile approximation.

[15] In [13] scintillator was irradiated with ^{137}Cs radioactive source with rate of 6 rad/s.

[16] For below discussion, the scintillator material and fiber density are assumed to be predefined on the basis of other considerations.

the dose accumulated, and λ_{geom} is determined by the design.

λ_{geom} reduction is profitable in a sense, that λ_{bulk} fall-off is less felt by the total scintillator tile light yield degradation. In order to decrease λ_{geom} one could shorten the mean light path of photon in non-irradiated tile. For illustration, considered is the shortening of mean light path achieved by worsening the quality of light reflection from tile edges. This would lead to lower radiation induced degradation effects from one hand, and to decreasing of the light yield from the other. Thus, having enough photostatistics, one would naively prefer the very poor light reflection efficiency from tile edges, if it were not for important transverse uniformity considerations (see [5]).

To prove λ_{geom} significant impact on the performance, and to get quantitative picture, three tiles of 4×4 cm^2 size with clear polished edges, with aluminized edges and with mat edges respectively, were irradiated with ^{60}Co source up to 2 $Mrad$ dose. Measured was the initial light yield after irradiation. The light yield losses in (%) versus accumulated dose are plotted in Figure 7. According to the expectations, the tile with clear polished edges shows the least degradation, and the tile with mat edges, and consequently the largest λ_{geom}, degrades to the highest extent. Results for different λ_{geom} values obtained in [11] and [16] also support our understanding of transparency impact on scintillator degradation. The above discussion is important in view of tile edge coverage choice, see [5].

Figures 8 and 9 illustrate **fiber degradation and annealing** effect for Bicron $BCF-91A$ and Kuraray $Y11(200)MS$ fiber samples after irradiation up to 5 $Mrad$ dose at shower maximum. Measured is the PM current vs. distance to PM for non-irradiated fiber sample, and for irradiated fiber sample in 7, 55, 175 and 2000 $hours$ after irradiation. Attenuation of signal from the largest distance for $BCF-91A$ fiber appeared to drop down to 20% from initial value. Subsequent annealing improves the attenuation up to 50% for the first $\sim$ 50 $hours$ with no further improvement. For $Y11(200)MS$ fibers the attenuation dropped to less than 10% value compared to the initial measurement. Annealing effect improves attenuation up to 40% for the first $\sim$ 50 $hours$ after irradiation and up to 70% after $\sim$ 175 $hours$ with no further improvement. Ku-

raray $Y11(200)MS$ fibers behaviour looks clearly more promising in view of LHCb dose rate. For smaller fiber length, $l \approx 25\ cm$, $Y11(200)MS$ fibers were shown to have much better radiation resistance compared to that of $BCF-91A$ fibers [17].

Translation of the dose collected to the **actual module degradation and** to the corresponding change in the **energy resolution** is done using Monte Carlo simulation studies. Critical here is the dose distribution along the module length, taken from Figure 3. For Monte Carlo calculations, all the radiation damage is assumed to have electromagnetic origination [17]. Using the relation between the "distance to PM" from Figures 8 and 9 and the dose accumulated, the dose dependence of attenuation length was estimated for Bicron $BCF-91A(DC)$ and Kuraray $Y11(200)MS$ fiber samples. Scintillator degradation was estimated using the information from Figures 6. Data distributions of scintillator brightness and fiber attenuation length vs. dose were fit with the exponent [18]. The fit gave [19] dose parameter for scintillator $D_S = 7.3\ Mrad$, and fiber dose parameters $D_F = 4.4\ Mrad$ for $BCF-91A(DC)$ fibers and $D_F = 7.1\ Mrad$ for $Y11(200)MS$ fibers [20], which were subsequently substituted to the Monte Carlo model [21].

The main results from Monte Carlo simulation of calorimeter performance degradation for $Y11(200)MS \oplus PSM-115$ and $BCF-91A(DC) \oplus PSM-115$ options are shown in Figures 10 and 11 respectively. Plotted are peak damage versus energy for accumulated dose of $0; 1; 2; 3; 4; 5\ Mrad$, energy resolution degradation for $5; 10; 20; 50; 100\ GeV$

[17] Hadronic component can result in higher damage effect, thus worsening the result.

[18] The assumed dependences of B_{Sci} and λ_{Fib} are

$$B_{Sci} = B^0_{Sci} \cdot e^{-\frac{D}{D_S}} \quad and \quad \lambda_{Fib} = \lambda^0_{Fib} \cdot e^{-\frac{D}{D_F}}\ ,$$

where B^0_{Sci} and λ^0_{Fib} are the values of B_{Sci} and λ_{Fib} before irradiation, and D is the accumulated dose.

[19] Note, that dose parameter estimates obtained correspond to LHCb scintillator tile geometry and fiber length.

[20] λ^0_{Fib} parameters for $BCF-91A(DC)$ and $Y11(200)MS$ fibers have almost equal values of 105 cm and 100 cm respectively.

[21] The simulation results were obtained for the LHCb module design.

energy, and

$$\frac{\sigma_{damage}}{E} = \sqrt{\left\{\frac{\sigma_E}{E}\right\}^2 - \left\{\left(\frac{\sigma_E}{E}\right)_0\right\}^2},$$

where subscript index "0" denotes non-irradiated value. The $\frac{\sigma_{damage}}{E}$ vs. dose dependence demonstrates the constant term degradation. For all the energies and all the dose values considered $BCF-91A(DC)\oplus PSM-115$ combination degrades stronger than that of $Y11(200)MS\oplus PSM-115$. Integral result is that constant term achieves 1.5% value [22] at 1.9 $Mrad$ accumulated dose for $BCF-91A(DC)\oplus PSM-115$ option. For $Y11(200)MS\oplus PSM-115$ combination constant term degrades to 1.5% under 2.2 $Mrad$ radiation dose.

At the same time Monte Carlo studies predict for the innermost modules to accumulate the dose of 2.5 $Mrad$ for 10 years of LHCb operation (Figure 2). As shown above, under this dose the constant term value is expected to exceed its limit of 1.5% after less than 10 years. Taking also into account Monte Carlo simulation uncertainty (mostly coming from the poorly known dose), the possibility to replace the innermost modules is foreseen in the calorimeter design [18].

6 Solution for LHCb

Radiation test at LIL was carried out with the working geometry, and is a proper base to make conclusions on. The best radiation hard $Y11(200)MS\oplus PSM-115$ combination was measured to loose 40% of light yield after irradiation with 2 $Mrad$ dose. Monte Carlo simulation studies show that this corresponds to the rise of constant term from 0.8% to 1.5%. This estimate is expected to be conservative, first of all because of high dose rate at the LIL test. Indications exist that scintillator sustains smaller degradation under LHCb dose accumulation rate. Nonetheless, in view of Monte Carlo simulation uncertainty, the possibility to replace ± 2 innermost module rows in x direction and ± 1 innermost module rows in y direction should be foreseen. The number of modules to be replaced does not critically depend on the Monte Carlo simulation uncertainty because

[22] Constant term of 1.5% is accepted as the limit of performance required.

of the sharp dose dependence on the distance to the beam axis. For the outer region with moderate radiation conditions either Kuraray $Y11(200)MS$ or Bicron fibers could be used.

Acknowledgements. It is a pleasure to thank E.Chevallay and LPI coordinator L.Rinolfi for their competent and friendly help in preparation to the experiment and during the samples irradiation, and the LIL crew for the excellent machine operation.

References

[1] LHCb Collaboration, LHCb Technical Proposal, CERN LHCC 98-4 LHCC/P4 20 February 1998.

[2] HERA-B Collaboration, HERA-B Proposal, DESY-PRC 94/02 May 1994; HERA-B Collaboration, HERA-B Design Report, DESY-PRC 95/01 January 1995.

[3] Bazilevsky A. *et al*, IEEE Transactions on Nuclear Science v.43, No.3 (1996).

[4] J.Badier *et al*, "Shashlik Calorimeter: Beam Test Results", Nucl.Instrum.Meth. A348 (1994) 74-86.

[5] S.Barsuk *et al*, "Fiber density and uniformity of response of LHCb electromagnetic calorimeter", LHCb 2000-034, CALO.

[6] S.Funaki *et al*, "Beam Test of Radiation Hardness of a Scintillating Tile/Fiber Calorimeter", Nucl.Instrum.Meth. A317 (1992) 123-134.

[7] S.W.Han *et al*, "Radiation Hardness Tests of Scintillating Tile/WLS Fiber Calorimeter Modules", Nucl.Instrum.Meth. A365 (1995) 337-351.

[8] A.Dorokhov, "Scintillator radiation damage", *presented at* LHCb calorimeter meeting, April 1999.

[9] CMS Collaboration, Technical Proposal, CERN LHCC 94-38 LHCC/P1 15 December 1994.

[10] Pribori i Tech. Exp., in Russian, 6 (1992) 95.

[11] Pribori i Tech. Exp., in Russian, 1 (1996) 1.

[12] ATLAS TILE CALORIMETER: Technical Design Report, by ATLAS Collab., CERN-LHCC-96-42, December 1996.

[13] Pribori i Tech. Exp., in Russian, 1 (1994) 86.

[14] "Radiation Hardness of Shashlik Type Calorimeter", CMS TN/96-133.

[15] Pribori i Tech. Exp., in Russian, 5 (1995) 85.

[16] Pribori i Tech. Exp., in Russian, 5 (1994) 58.

[17] E.Tarkovsky, "The HERA-B electromagnetic calorimeter", Nucl.Instrum.Meth. A379 (1996) 515.

[18] S.Barsuk *et al*, "Design and construction of electromagnetic calorimeter for LHCb experiment", LHCb 2000-043, CALO.

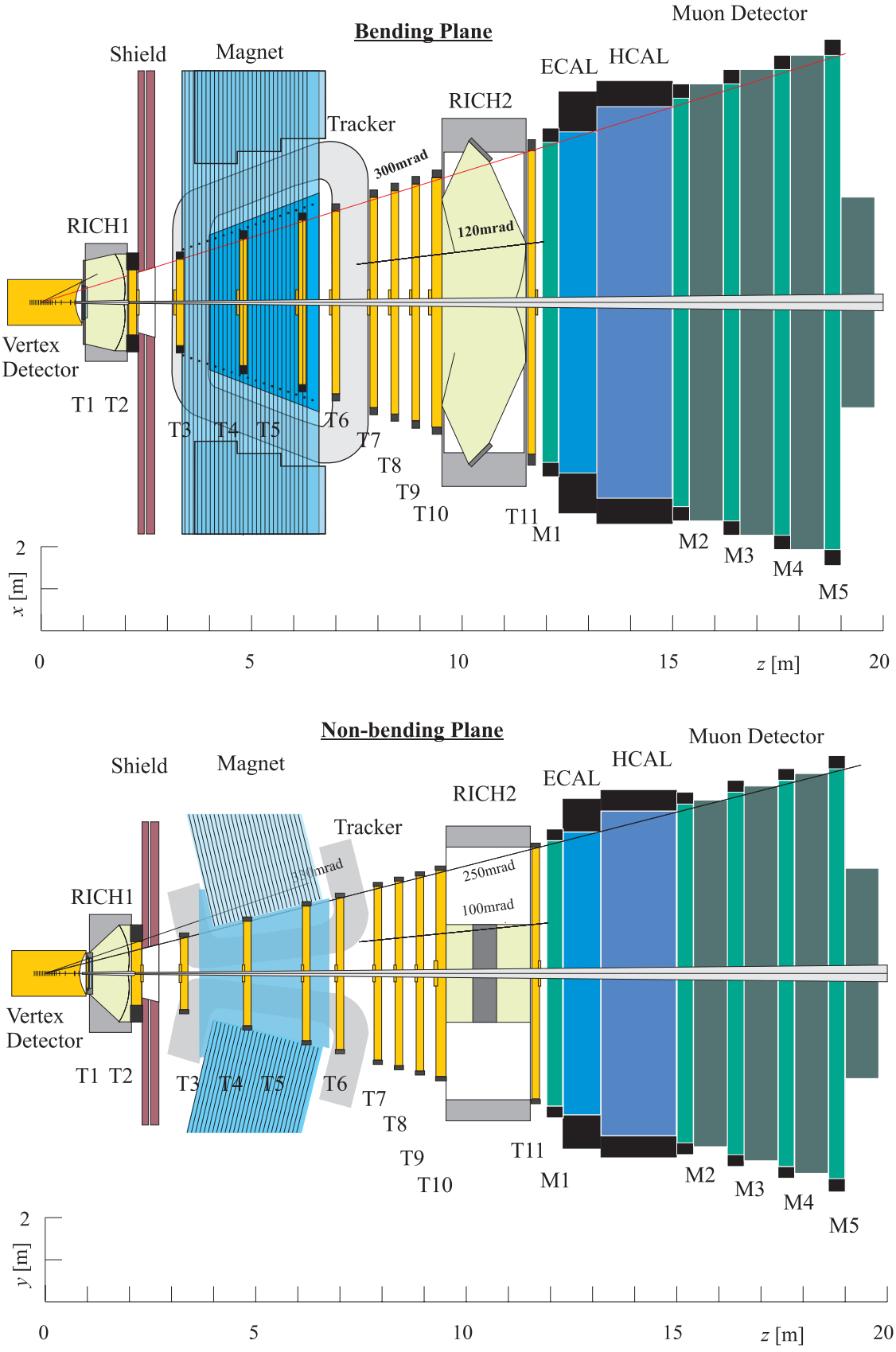

Figure 1: *LHCb detector*

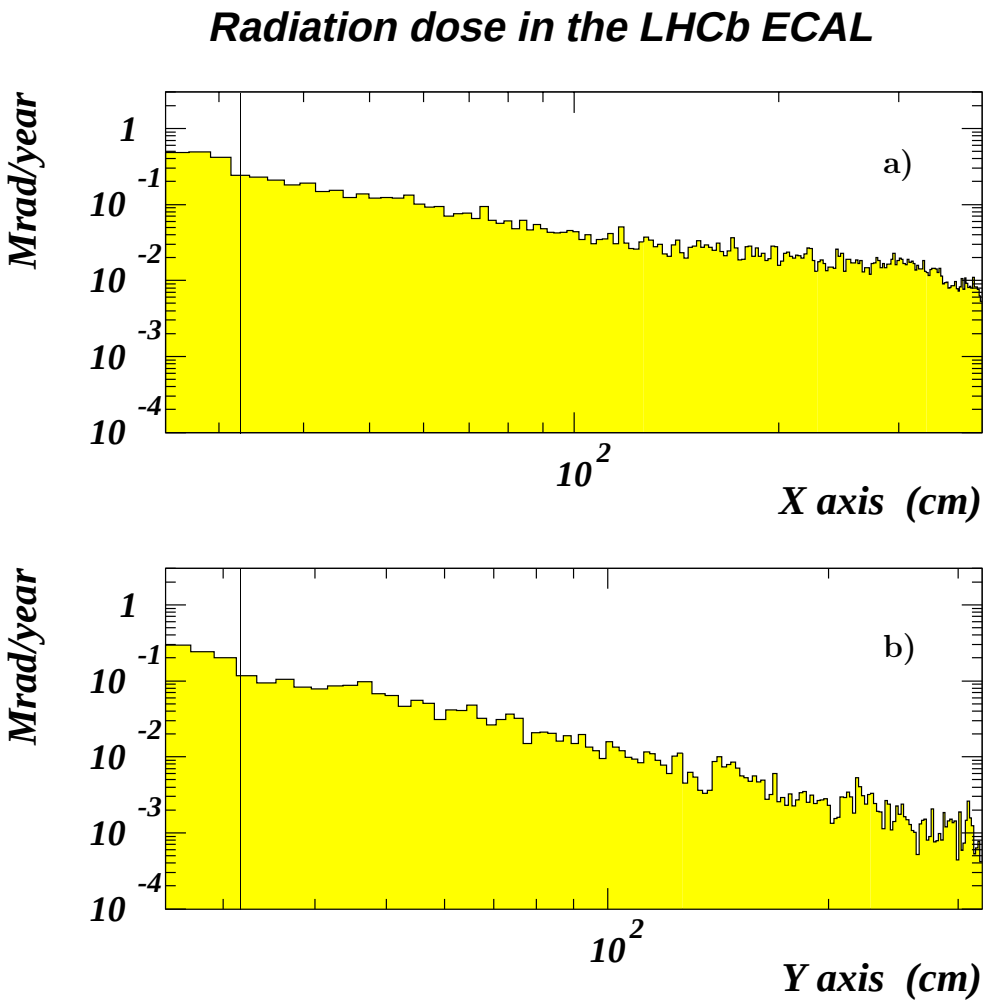

Figure 2: *The expected annual radiation dose distribution along x-axis in $y = 0$ slice (* **a** *) and along y-axis in $x = 0$ slice (* **b** *). Vertical lines indicate the innermost position of active calorimeter volume*

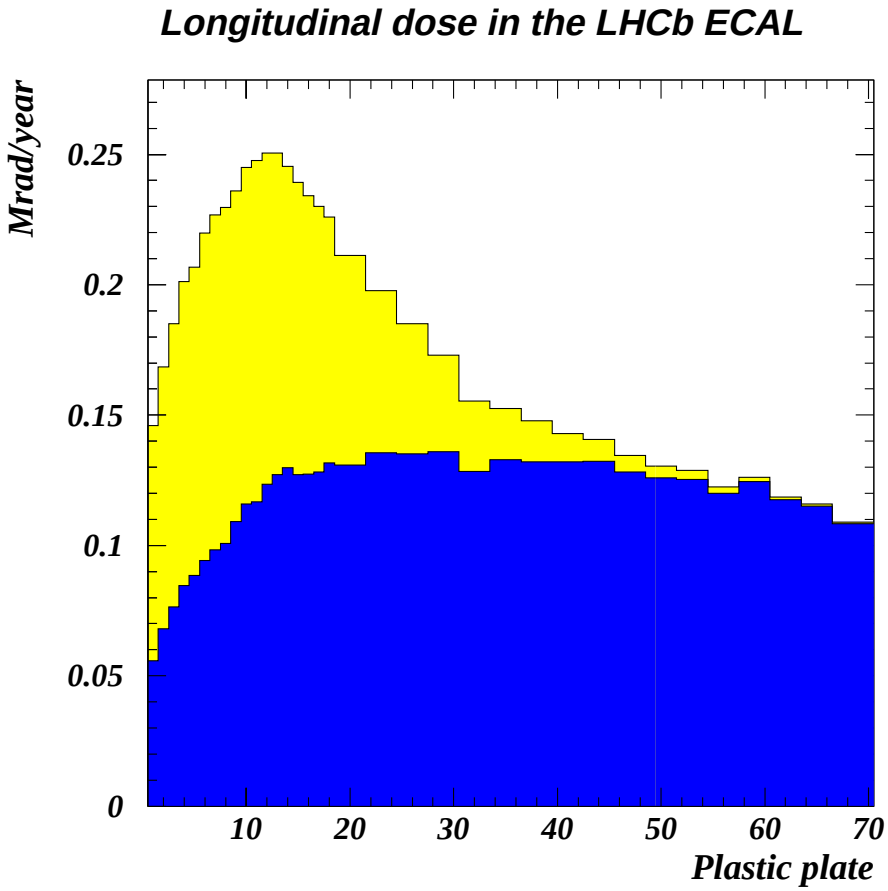

Figure 3: *The longitudinal profile of dose for the innermost module. The contributions from electromagnetic and hadronic components of the shower are shown separately*

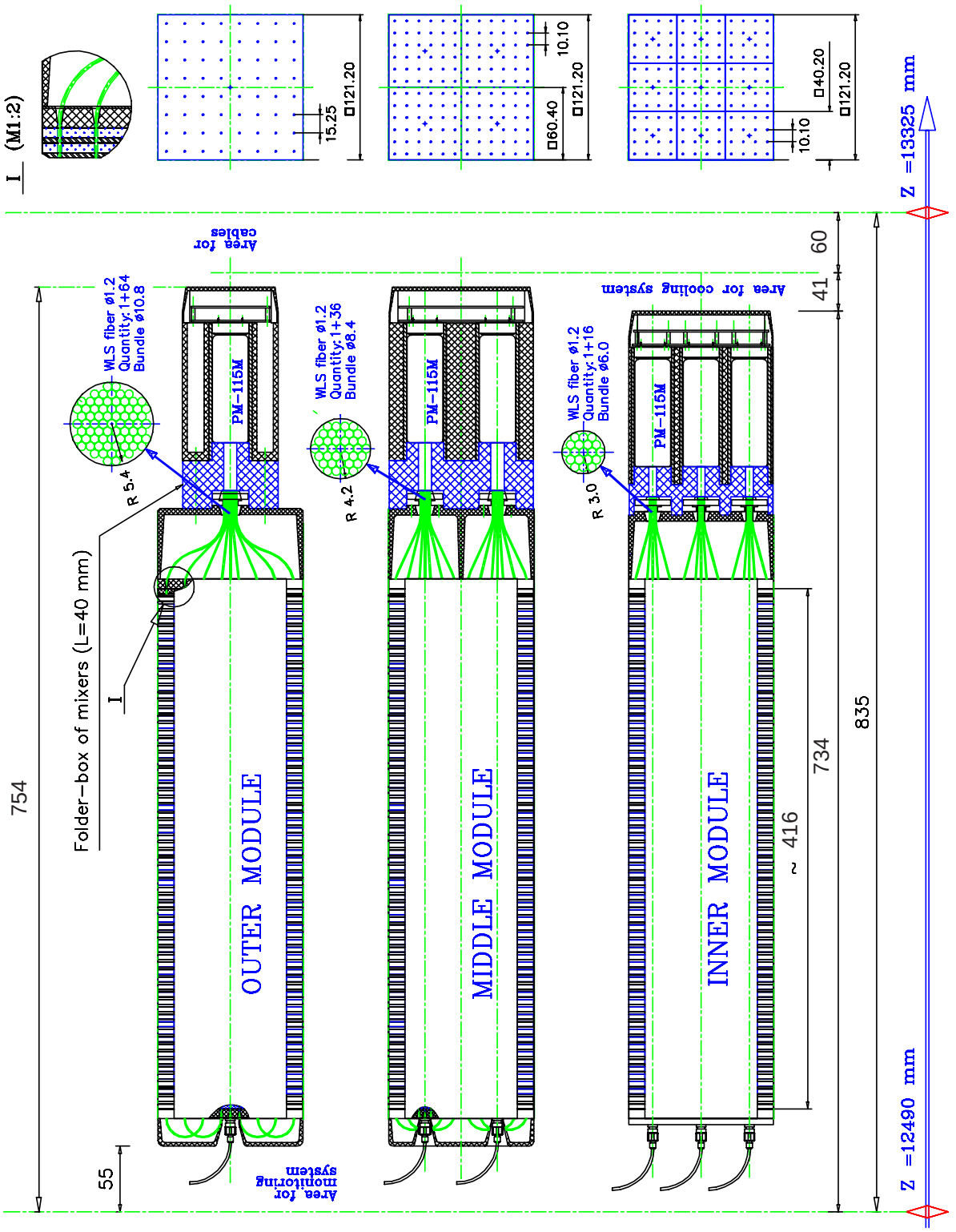

Figure 4: *Electromagnetic calorimeter modules for inner, middle and outer sections. At the monitoring side shown are transport fibers, connectors, fiber loops (if any) and plastic covers. At the read-out side shown are fiber bundles, PMs and their bases. Also shown are area for splitters, space for cooling system and for cabling, and the related mechanics*

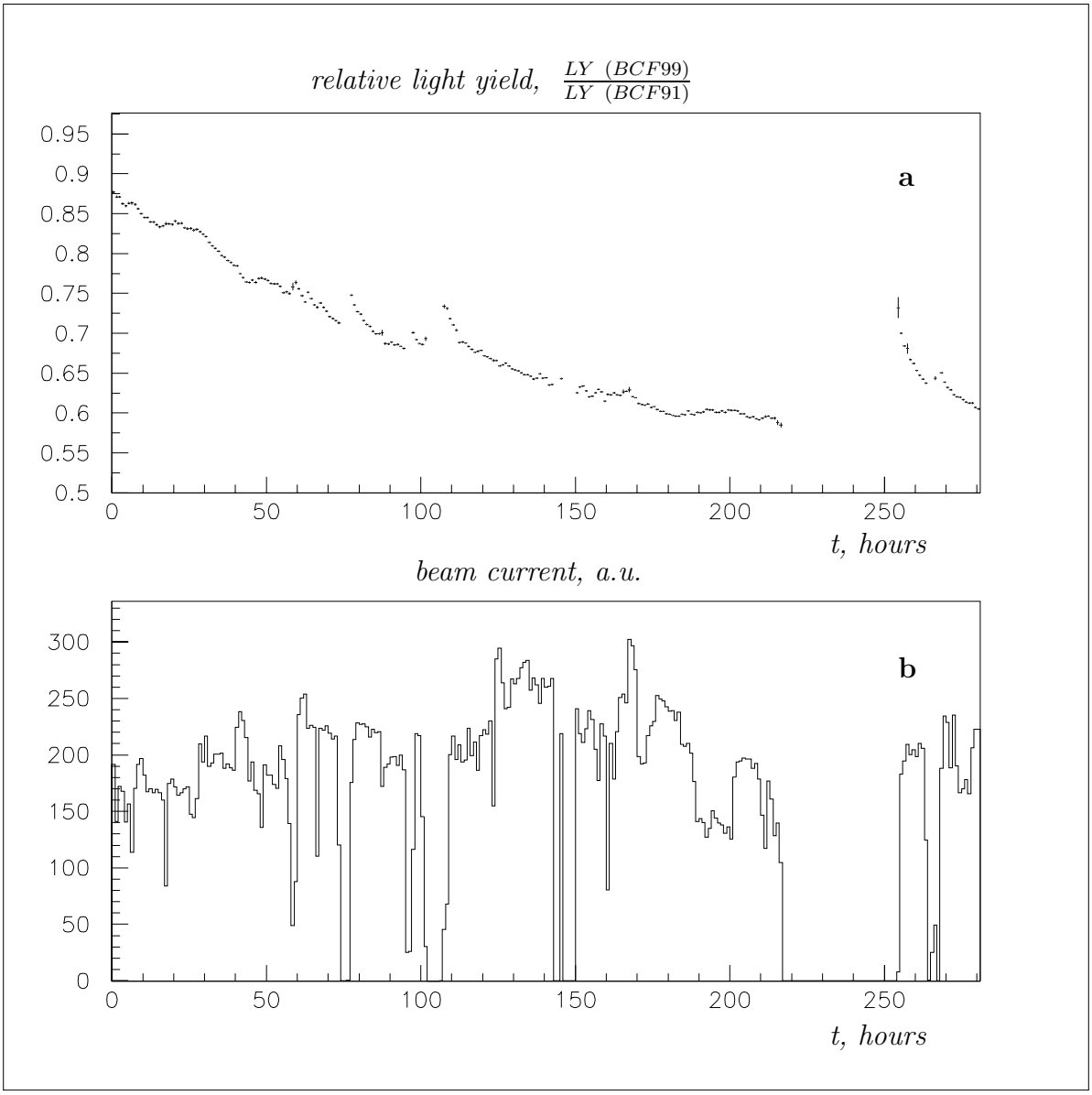

Figure 5: *BCF*99 *fibers degradation dynamics relative to the degradation of* $BCF91$ *fibers under irradiation up to* 0.5 $Mrad$ *with ITEP accelerator. Shown is the time dependence of relative light yield, (* $\frac{LY\ (BCF99)}{LY\ (BCF91)}$ *), (* **a** *); and the corresponding beam current (* **b** *)*

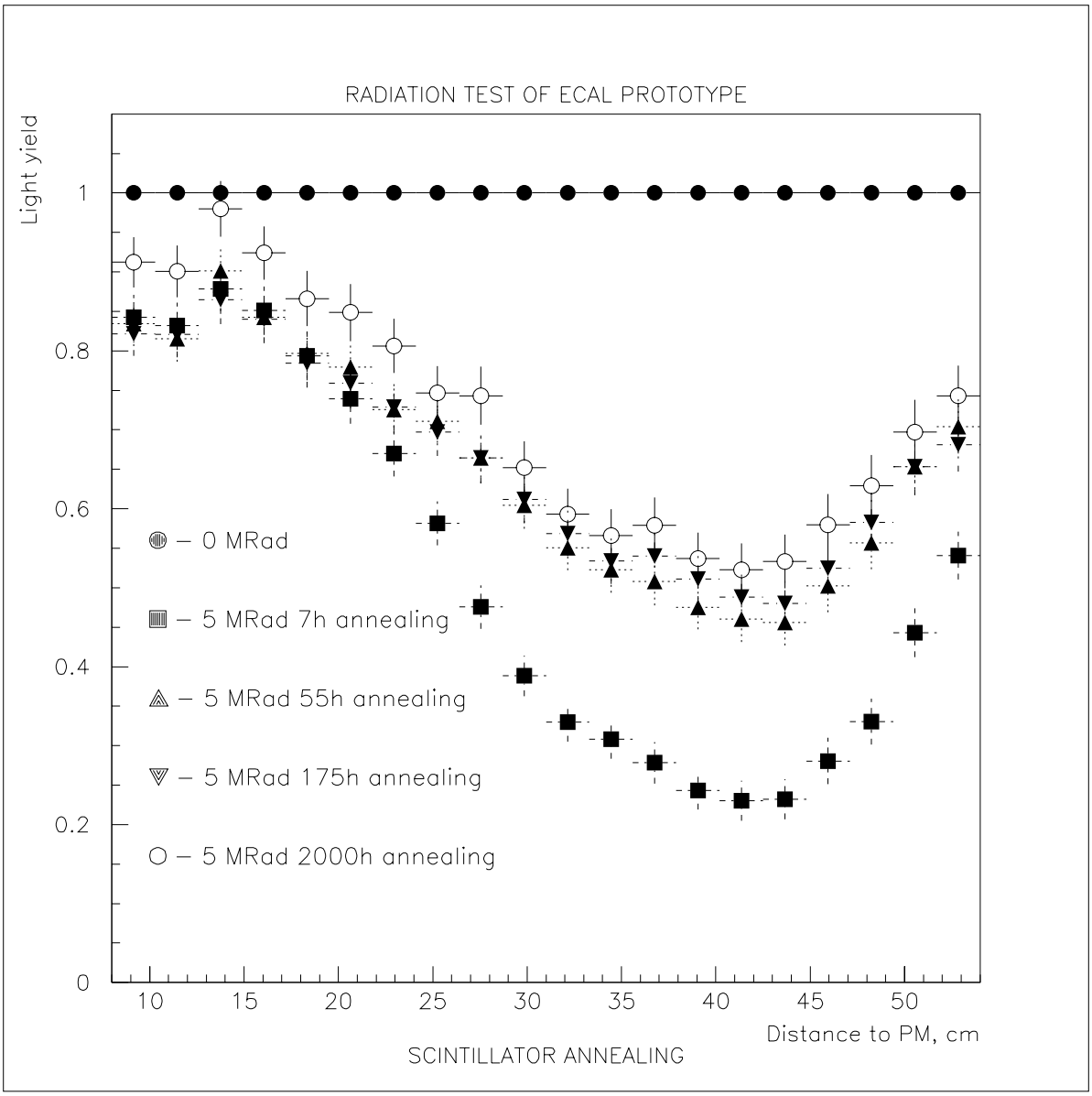

Figure 6: *Scintillator degradation and annealing effect after irradiation at LIL up to* 5 *Mrad dose at shower maximum (shower maximum position corresponds to distance to PM of* 42 *cm). Shown is the light yield vs. distance to PM after* 7, 55, 175 *and* 2000 *hours after irradiation*

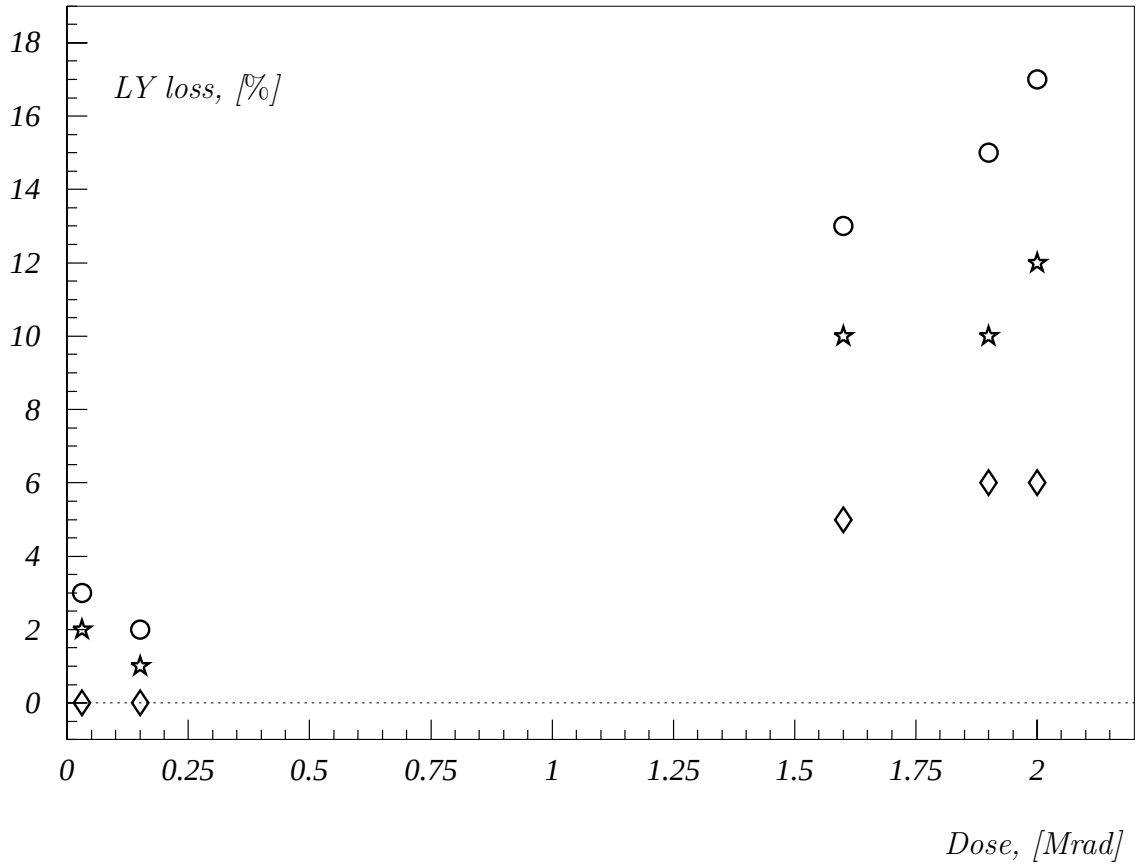

Figure 7: *Radiation induced degradation of tiles of* 4×4 cm^2 *size with open (diamond), aluminized (stars) and mat (circles) edges. Shown is the light yield losses (%) vs. accumulated dose. Tiles were irradiated with* ^{60}Co *source up to* 2 $Mrad$ *dose, and read out by WLS fibers. Typical error of each measurement is* $\sim 2\%$

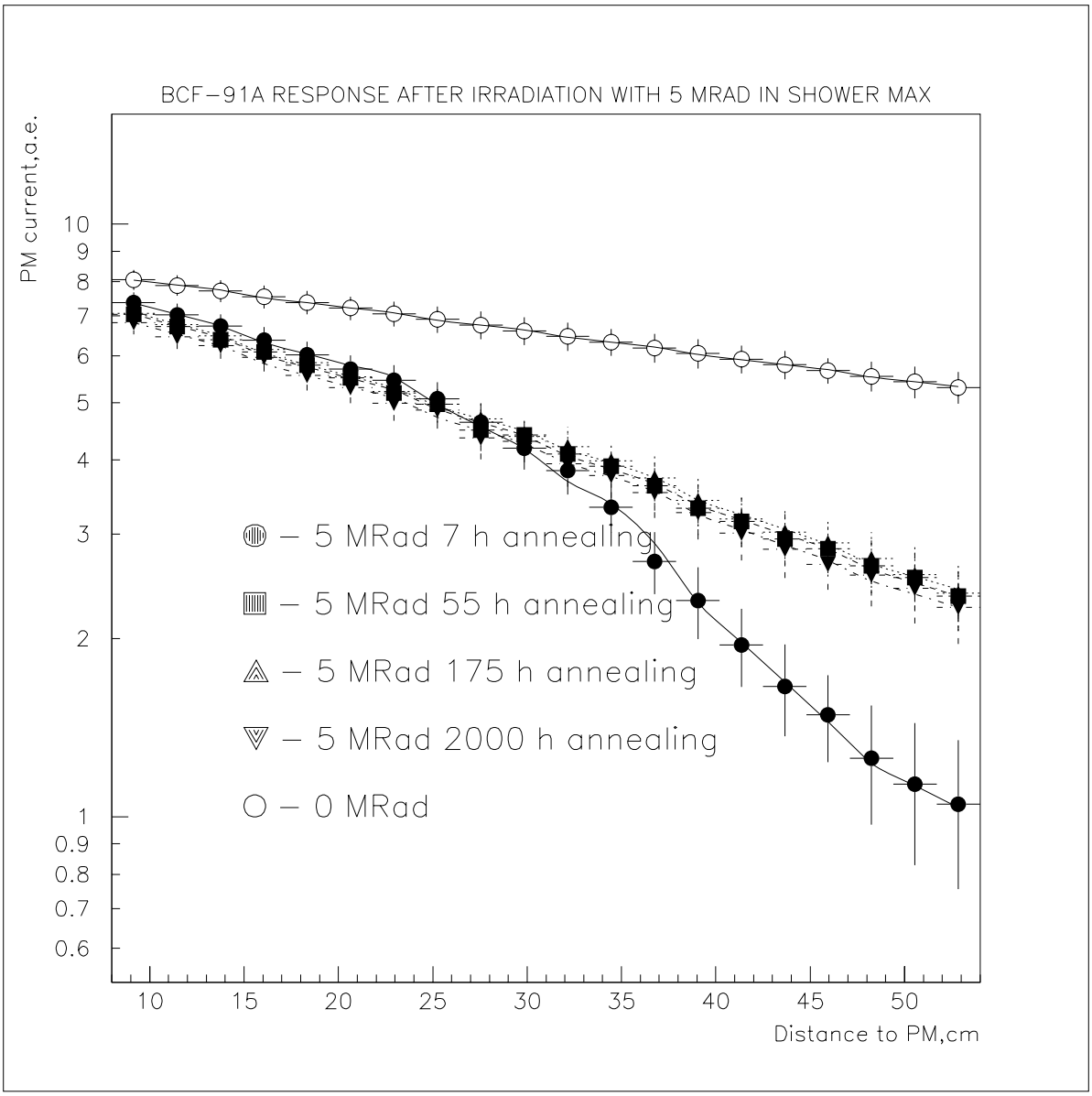

Figure 8: *Bicron* $BCF-91A$ *fiber degradation and annealing effect after irradiation at LIL up to* 5 $Mrad$ *dose at shower maximum. Shown is the PM current vs. distance to PM for non-irradiated fiber sample, and for irradiated fiber sample after* 7, 55, 175 *and* 2000 *hours after irradiation*

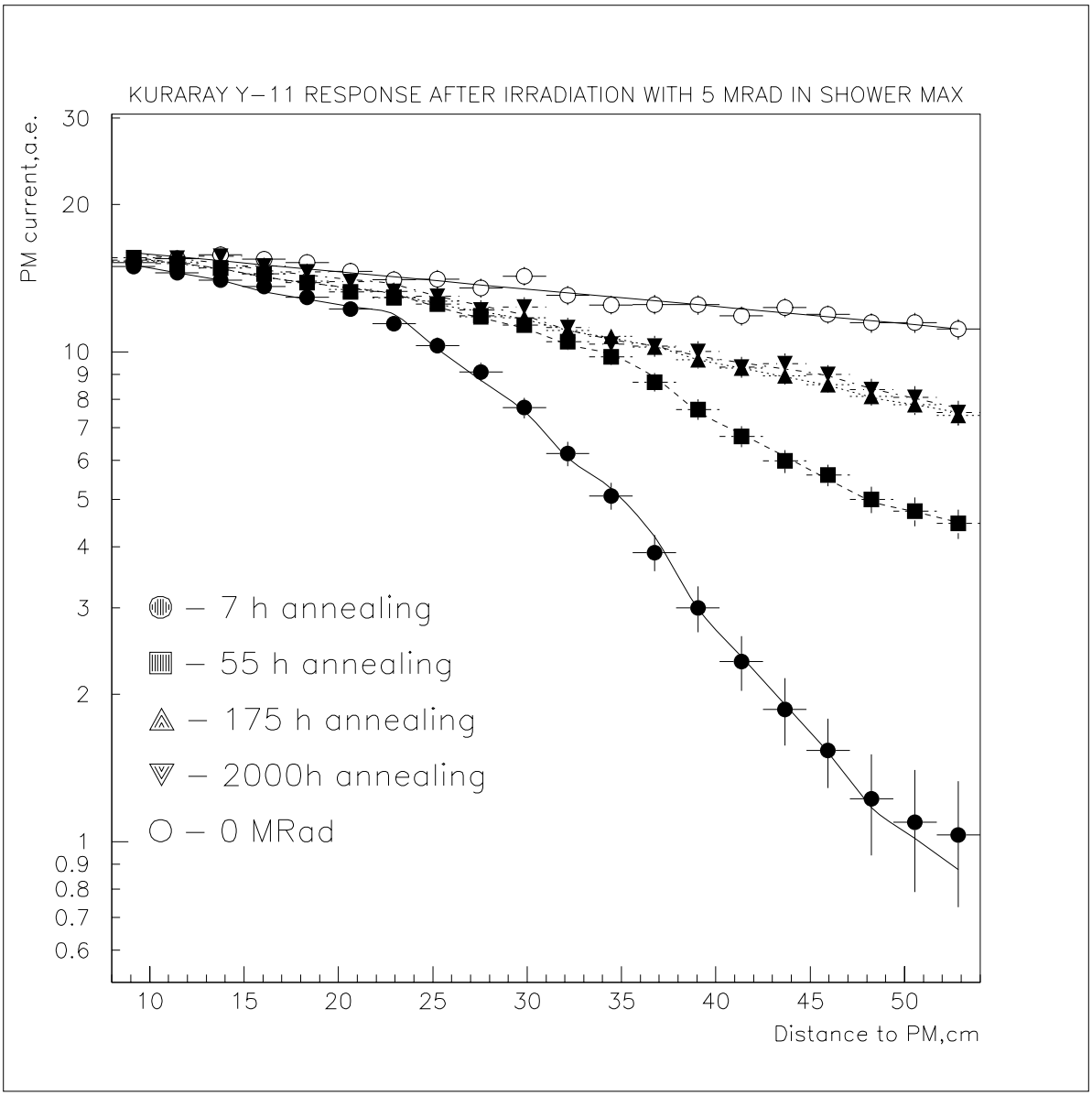

Figure 9: *Kuraray Y*11(200)*MS fiber degradation and annealing effect after irradiation at LIL up to* 5 *Mrad dose at shower maximum. Shown is the PM current vs. distance to PM for non-irradiated fiber sample, and for irradiated fiber sample after* 7, 55, 175 *and* 2000 *hours after irradiation*

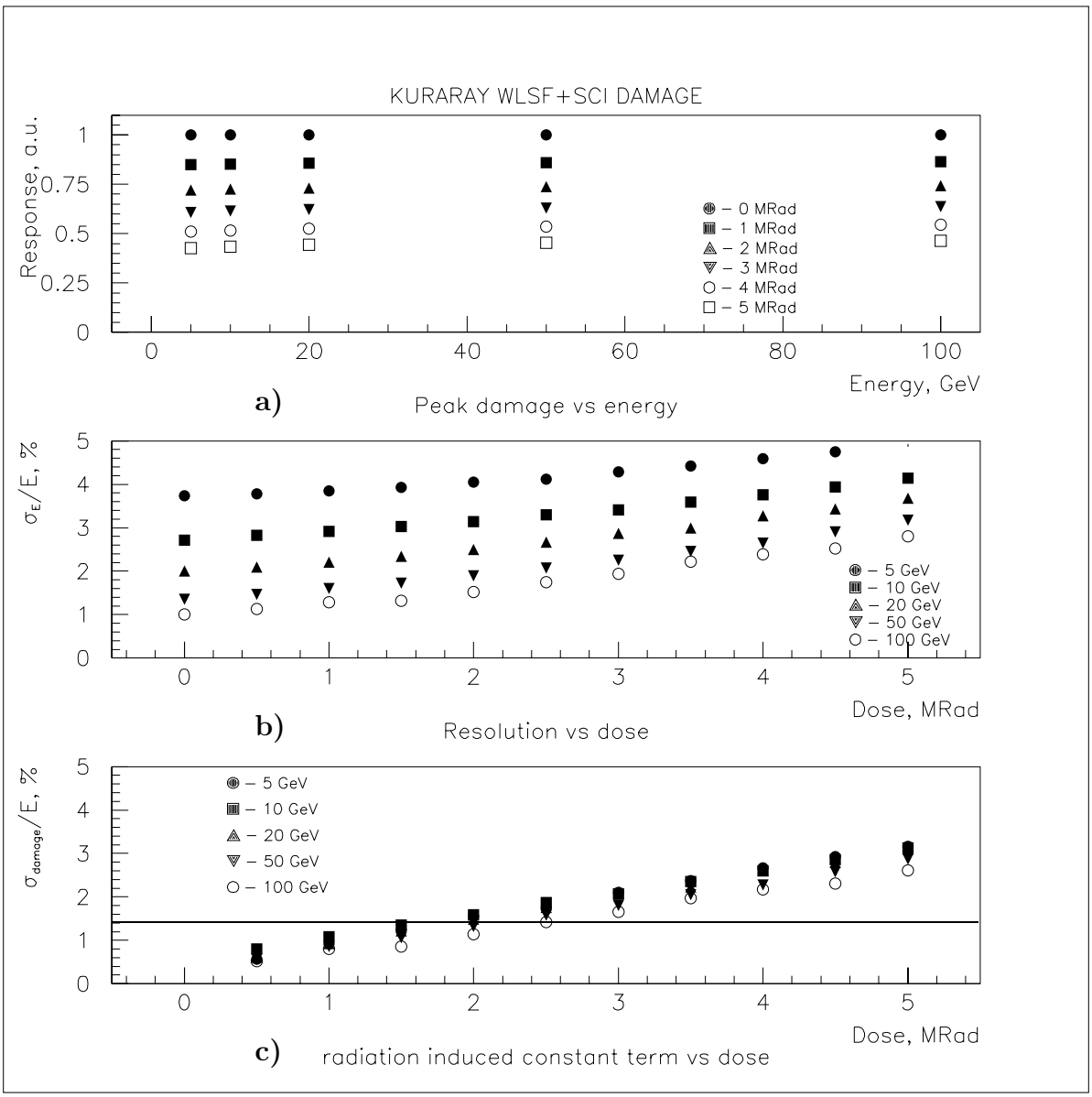

Figure 10: *Monte Carlo simulation studies of radiation induced module performance degradation.* $Y11(200)MS \oplus PSM - 115$ *combination and dose profile from Figure 3 is considered. Shown are peak damage versus energy for accumulated dose of* $0; 1; 2; 3; 4; 5$ $Mrad$ *(* **a** *); energy resolution degradation for* $5; 10; 20; 50; 100$ GeV *energy (* **b** *); constant term degradation for* $5; 10; 20; 50; 100$ GeV *energy (* **c** *). Horizontal line corresponds to the* 1.5% *value of the constant term. For details see the text*

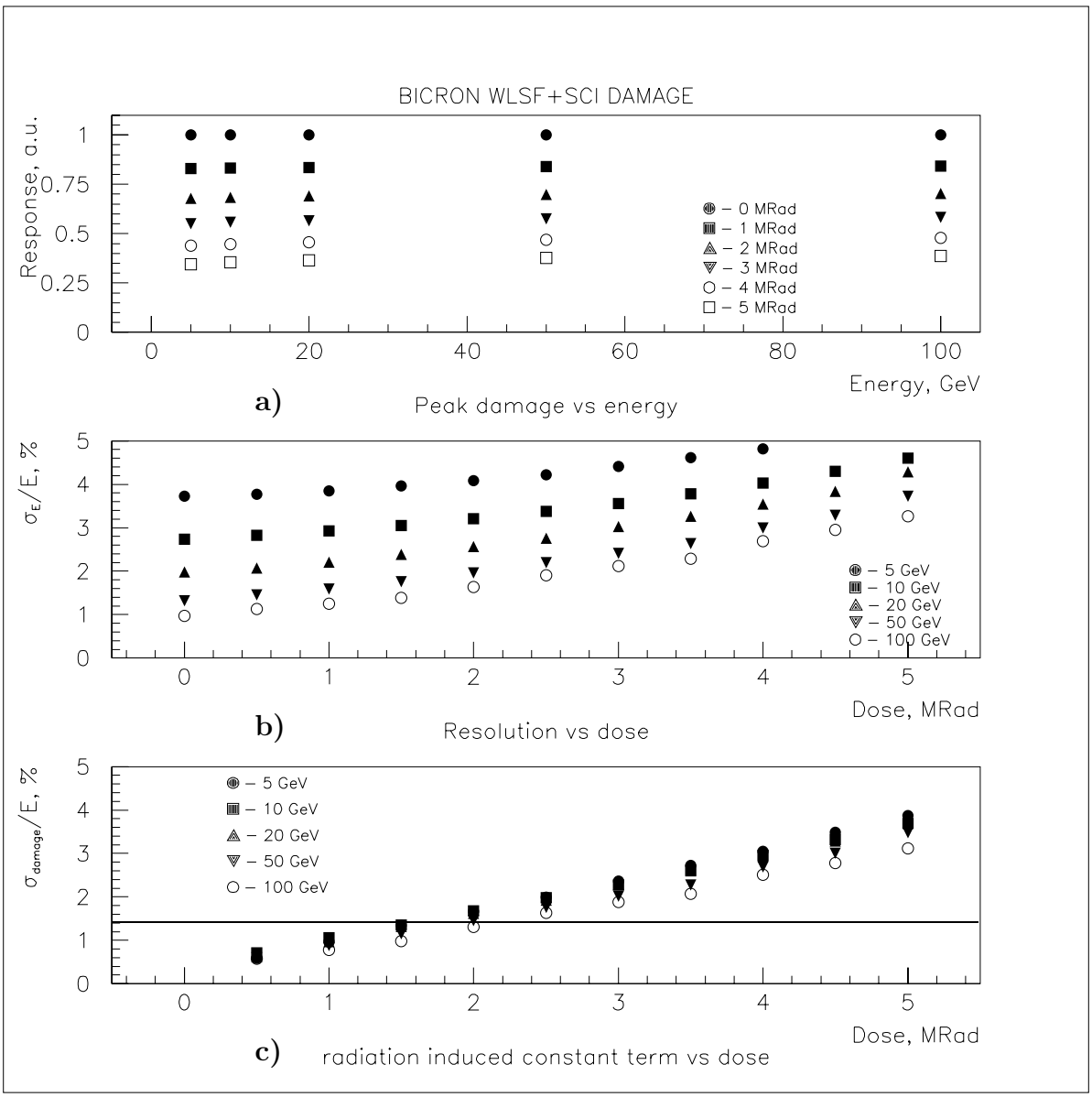

Figure 11: *Monte Carlo simulation studies of radiation induced module performance degradation.* $BCF-91A(DC)\oplus PSM-115$ *combination and dose profile from Figure 3 is considered. Shown are peak damage versus energy for accumulated dose of* $0;1;2;3;4;5$ $Mrad$ *(* **a** *); energy resolution degradation for* $5;10;20;50;100$ GeV *energy (* **b** *); constant term degradation for* $5;10;20;50;100$ GeV *energy (* **c** *). Horizontal line corresponds to the* 1.5% *value of the constant term. For details see the text*